Dynamic Scheduling of Internal Exhaust Gas Recirculation Systems.

Anna G. Stefanopoulou and Ilya Kolmanovsky
Ford Research Laboratory
2000 Rotunda Dr., MD 2036, Dearborn, MI 48121
astefano@ford.com and ikolmano@ford.com

Abstract

In this paper we analyze the nonlinear dynamic behavior of an internal exhaust gas recirculation system based on the mean-value model of an experimental engine equipped with a camshaft phaser. We develop a dynamic camshaft timing schedule that regulates the internal exhaust gas recirculation system while maintaining transient engine torque response similar to an engine with zero exhaust gas recirculation. The dynamic schedule consists of a steady-state map of the camshaft timing for optimum exhaust gas recirculation based on throttle position and engine speed, and a first order lag that regulates the transition of the camshaft timing to the optimum point. A scheme for adjusting the time constant of the first order lag depending on engine speed and throttle position is described.

1. Introduction

Exhaust gas recirculation (EGR) was introduced in the early 1970s to reduce the formation of oxides of nitrogen (NO_x) in internal combustion engines. The inert exhaust gases dilute the inducted air-fuel charge and lower the combustion temperature which reduces NO_x feedgas emissions. Conventionally, exhaust gas recirculation is accomplished by controlling the exhaust gas that is supplied from the exhaust manifold to the intake manifold through a vacuum actuated valve. The EGR control algorithm is a simple PI or PID loop that adjusts the valve position to the scheduled steady-state value. Exhaust gas recirculation alters the breathing process dynamics and consequently the torque response. Careful steady-state and transient control design is necessary to maintain good engine torque response. For this reason, EGR is typically turned off or is considerably delayed in transient engine operations, engine warm-up, and idling.

The advances in real-time computing and hardware are making possible the application of fully controlled valve events. Optimized valve events can improve the gas exchange process and enable control of internal EGR. Variable camshaft timing is an innovative and simple mechanical design approach for controlling EGR. By retarding the camshaft timing, combustion products which would otherwise be expelled during the exhaust stroke are retained in the cylinder during the subsequent intake stroke. This is a method of phasing the camshaft to control residual dilution and achieve the same results as with the conventional external EGR system, thus providing an innovative solution to an old problem.

Achieving exhaust gas recirculation through the exhaust manifold during the intake stroke is a better way of controlling the residual mass fraction during transients because (i) we eliminate the long transport delay associated to the exhaust-to-intake manifold path, and (ii) we bypass the slow dynamics associated with the intake manifold filling dynamics. Fast transient control of the internal exhaust gas recirculation (IEGR) is only limited by the camshaft phasor dynamics and computational delays. At a first glance, this suggests a possibility of better transient control of feedgas emissions than can be achieved with the conventional external exhaust gas recirculation (EEGR). Analysis of the IEGR system in throttled engines shows, however, that the IEGR system interacts with the slow intake manifold filling dynamics and can cause, in fact, unacceptable engine performance.

In this paper we analyze the nonlinear dynamic behavior of the IEGR system based on the mean-value model of an experimental engine equipped with a camshaft phaser. We develop a dynamic camshaft timing schedule that regulates IEGR while maintaining transient engine torque response similar to an engine with zero EGR. The torque response of an engine with zero EGR provides the benchmark for the engine performance that we wish to achieve because any level of EGR can cause severe torque hesitation if not well calibrated.

Modularity of the IEGR control function is another very important requirement for the control design. Modular IEGR control function will allow its rapid implementation in existing real-time engine controllers. For this reason, the IEGR controller architecture that we develop can be seamlessly added or removed from the pow-

ertrain controller depending on the platform needs. Figure 1 shows the developed IEGR control architecture. We dynamically schedule the camshaft timing (CT) that regulates IEGR based on the measured throttle angle (θ_m) and engine speed (N). Briefly stated here, the dynamic schedule consists of (i) the steady-state camshaft timing values (CT) for all throttle and engine speeds, and (ii) the time constant (τ_{ct}) of the first order differential equation that defines the transient behavior of IEGR from one steady-state point to the next. The time constant is adjusted using a nonlinear static feedback of engine speed and throttle position as to meet the torque response requirements.

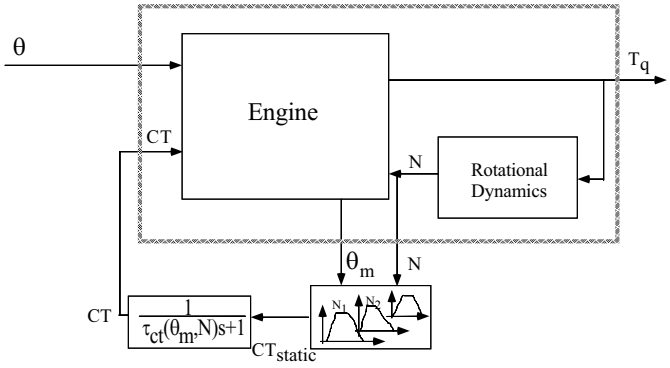

Figure 1: Control structure of the internal EGR system.

2. Internal EGR System

The mean-value model of an experimental engine with variable camshaft timing shows that significant NO_x reduction can be achieved by allowing the exhaust valve to remain open for a longer period of time during the intake stroke. This is achieved by increasing the fraction of exhaust gases that remain into the cylinder and lower the combustion temperature during the subsequent cycle. Figure 2 shows the correlation between NO_x formation and percentage of external EGR flow in a conventional engine. Similarly, Figure 3 shows the effects of camshaft timing (CT) to the feedgas NO_x generation in an IEGR engine. Retarding camshaft timing increases the internal exhaust gas recirculation (IEGR) and that results in reduction in feedgas NO_x[1]. From Figure 3 it is obvious that to reduce feedgas NO_x we have to ensure engine operation with maximum CT.

At the same time CT lowers the volumetric efficiency of the engine as shown in Fig. 4 allowing less mass of fresh air into the cylinders. The mean mass flow rate of fresh air into the cylinders $\dot{m}_{cyl}$ is a function of volumetric efficiency (η), the intake manifold density (ρ_m), the engine

[1]The simple relationship "increasing camshaft timing (CT) increases IEGR" is used throughout this paper. A mathematical equation describing the relationship between CT and IEGR is not available because it is difficult to measure EGR mass inside the cylinder.

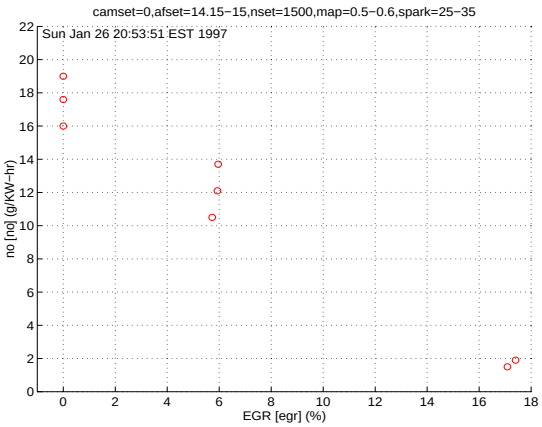

Figure 2: Effects of external exhaust gas recirculation (EGR) to feedgas NO_x.

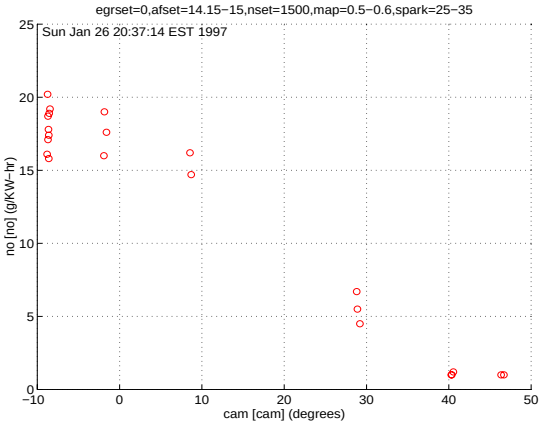

Figure 3: Effects of camshaft timing (CT) to feedgas NO_x.

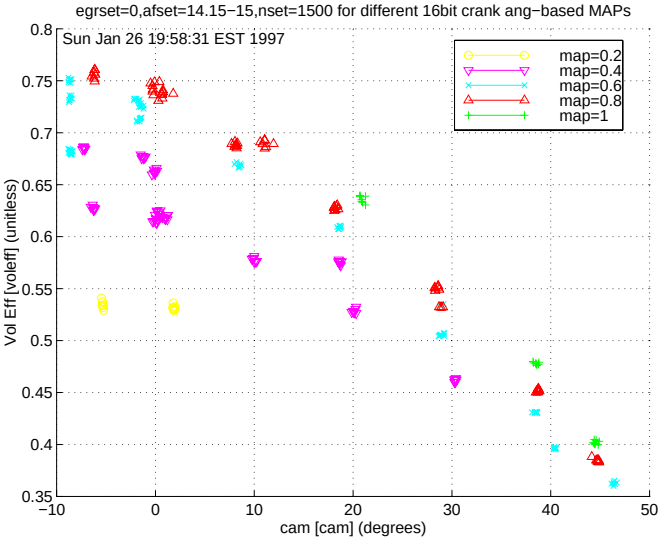

Figure 4: Volumetric efficiency as a function of camshaft timing for different manifold pressures at 1500 RPM.

displacement (V_d), and engine speed (N):

$$\dot{m}_{cyl} = \eta \rho_m V_d \frac{N}{120} \ . \tag{1}$$

Using the continuity equation for air flow into ($\dot{m}_\theta$) and out ($\dot{m}_{cyl}$) of the intake manifold, and the ideal gas law assuming constant air temperature (T_m)[2] we describe the intake manifold pressure (P_m):

$$\frac{d}{dt} P_m = K_m (\dot{m}_\theta - \dot{m}_{cyl}) \ . \tag{2}$$

The air flow into the intake manifold ($\dot{m}_\theta$) can be computed by the discharge coefficient at the throttle plate ($A(\theta)$) and the pressure difference across the throttle plate ($\frac{P_{ambient}}{P_m}$). Using the regression equations in [Stefanopoulou et. al. 1995] we can describe the breathing process of the IEGR system:

$$\begin{aligned} \dot{m}_\theta &= F_1(P_m, \theta) \\ \frac{d}{dt} P_m &= K_m (\dot{m}_\theta - \dot{m}_{cyl}) \\ \dot{m}_{cyl} &= F_2(CAM, P_m, N) \ . \end{aligned} \tag{3}$$

In-cylinder torque generation can be simply computed using an empirical function of the mass air flow into the cylinder ($\dot{m}_{cyl}$), the air-to-fuel ratio (A/F), the spark timing (σ), and the engine speed (N):

$$T_q = F_3(\dot{m}_{cyl}, \sigma, N, A/F) \tag{4}$$

Our goal is to schedule IEGR without detrimental consequences to engine torque response. For simplicity, we will assume precise air-to-fuel ratio and spark control. We will also analyze the effects of IEGR on engine torque response assuming constant engine speed and schedule IEGR as a function of engine speed. With these two assumptions, the engine torque response becomes equivalent to the mass air flow into the cylinder.

3. Static Schedule

Exhaust gas recirculation decreases the engine torque response. Figure 5 shows the normalized torque response for zero IEGR (dashed line) and for the maximum IEGR (dashed-dot line) that the engine can achieve. The normalized torque is given as a function of throttle angle for constant engine speed. To minimize feedgas emissions we need to operate at maximum IEGR. To ensure maximum torque at wide open throttle (WOT) we need to reduce IEGR back to zero. The solid line in Figure 5 shows such a smooth transition from maximum IEGR for part throttle to zero IEGR for WOT. For very small throttle angles (small air flow into the cylinders) IEGR deteriorates the combustion stability because of the high level of dilution. IEGR, therefore, is scheduled at zero for small throttle angles to maintain combustion stability. Using the above guidelines we derive the static camshaft timing (CT_{static}) as follows: (1) near idle it is scheduled for idle stability which requires cam phasing equal to zero; (2) at mid-throttle it is scheduled for emissions which favors fully retarded cam phasing; and (3) at wide open throttle (WOT) it is scheduled for maximum torque which requires camshaft timing to be advanced back to 0 degrees. The developed camshaft scheduling scheme, shown

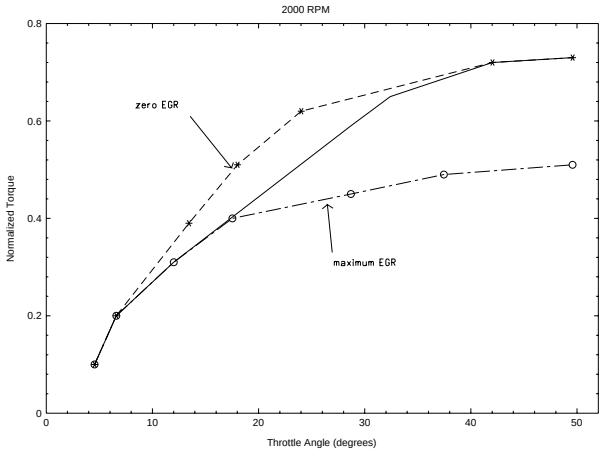

Figure 5: Comparison between static normalized torque response for zero IEGR, maximum IEGR, and a realizable IEGR scheme.

in Fig. 6, ensures reduction of feedgas emissions under the constraint of smooth steady state torque response for engine speed equal to 2000 RPM.

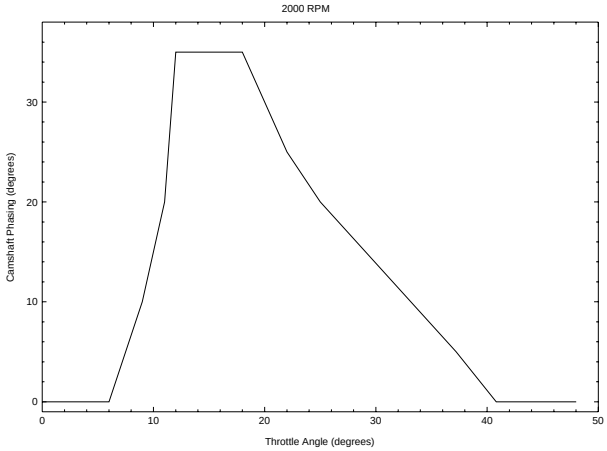

Figure 6: The static camshaft scheduling scheme at 2000 rpm.

This steady-state map can be derived based on different static optimization schemes depending on static engine performance tradeoffs that satisfy design require-

[2] In contrast to the conventional EGR systems, the internal exhaust gas recirculation system described in this paper maintains constant intake manifold temperature for different level of EGR recirculation. This happens because, the exhaust gas recirculation is achieved through the exhaust manifold and not the intake manifold.

ments. We chose pedal position and engine speed as inputs to this map to allow modular implementation of the control strategy. Throttle position is a natural independent variable for the camshaft control scheme. Engine speed, although not independent, is a slowly varying parameter, which implies that it can be safely used as the second scheduling parameter. The problem that remains unsolved is the transition characteristics from one static IEGR point to the next set point as the steady-state map requires. To minimize feedgas emissions we want to change camshaft timing (CT) to the optimum position (CT_{static}) as fast as possible or as fast as the actuator bandwidth allows.

4. Analysis of Transient Torque Response

We first analyze the effects of the IEGR dynamics on the transient torque response of the engine. As in the previous section, we assume a tight air-fuel ratio and spark control loop which implies that the torque response is determined by the airflow response.

Figure 7 shows the torque response of the IEGR engine to an instantaneous throttle change for the two constant engine speed values of 750 rpm and 2000 rpm. When the throttle angle changes instantaneously at $t = 0$ to a new value θ_m, the CT changes to a new value, $CT_{static}(\theta_m, N)$, according to

$$\begin{aligned} CT(t) = \quad & (1 - \exp(-t/\tau_{ct}))CT_{static}(\theta_m, N) \\ & + \exp(-t/\tau_{ct})CT(0), \ t \geq 0. \end{aligned} \tag{5}$$

The three different torque profiles in Figure 7 result for the three different values of τ_{tc}. If the CT changes fast (τ_{tc} is small) the torque response may exhibit an undershoot. This happens because of the tendency of the airflow to decrease with the increase in CT. If the CT changes slowly (τ_{tc} is large) the torque may overshoot. This happens because the airflow first increases quickly due to the intake pressure dynamics caused by a larger throttle angle; then the airflow decreases due to the CT slowly approaching the desired, larger than the initial, value. From the driver's perspective both, the undershoot and the overshoot, are undesirable.

The above intuitive arguments showing that the speed of CT adjustment affects the engine torque response can be supported analytically. The linearization of Equation 4 results in:

$$\begin{aligned} \Delta\dot{m}_\theta &= k_{\theta 1}\Delta\theta - k_{\theta 2}\Delta P_m \\ \Delta\dot{m}_{cyl} &= -k_{p1}\Delta CT + k_{p2}\Delta P_m \\ \frac{d}{dt}\Delta P_m &= k_m(\Delta\dot{m}_\theta - \Delta\dot{m}_{cyl}) \ , \end{aligned} \tag{6}$$

where $k_{\theta i} > 0, k_{pi} > 0$ for $i = 1, 2$ and $k_m > 0$. The transfer function between camshaft timing, throttle position, and mass air flow into the cylinders is given by:

$$\Delta\dot{m}_{cyl} = \frac{k_m k_{\theta 1} k_{p2}}{s + k_m(k_{\theta 2} + k_{p2})}\Delta\theta - \frac{k_m k_{p1} k_{\theta 2} + k_{p1} s}{s + k_m(k_{\theta 2} + k_{p2})}\Delta CT \ . \tag{7}$$

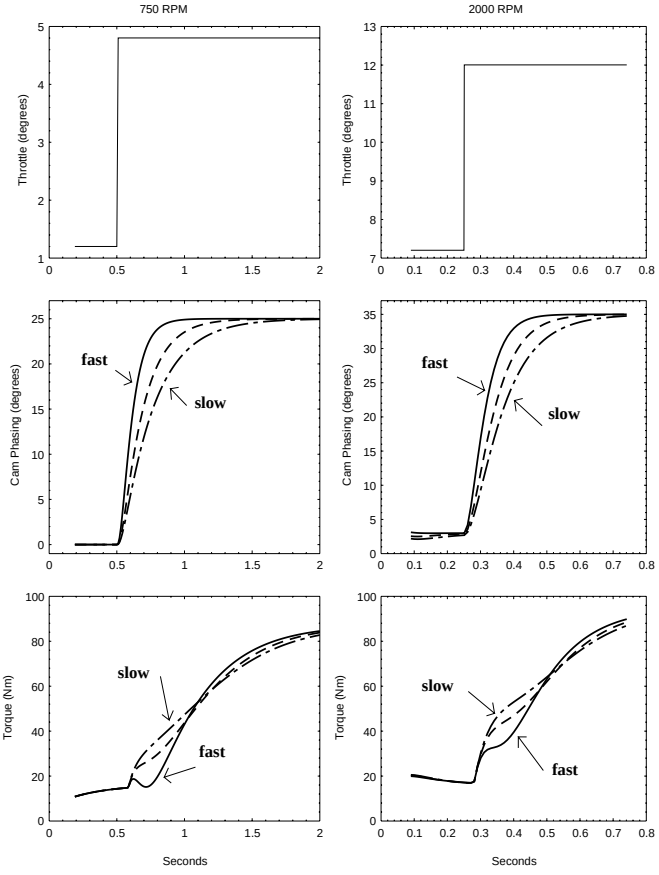

Figure 7: Torque response (at 750 and 2000 RPM) using different camshaft dynamic characteristics.

Linearization of the dynamic camshaft timing scheme results in :

$$\Delta CT = \frac{k_o}{\tau_{ct}s + 1}\Delta\theta \tag{8}$$

where $k_o = \frac{\partial(CT_{static})}{\partial\theta}$ depends on throttle angle and engine speed. The gain k_o in contrast to all the other gains (k_i's) takes positive and negative values based on the different operating regimes as described in Section 3. and shown in Fig. 6. Substitution of the linear camshaft scheduling scheme to Eq. 7 results in the transfer function from throttle angle to cylinder air flow for the closed loop IEGR system.

$$\begin{aligned} \Delta\dot{m}_{cyl} &= \left[\frac{k_m k_{\theta 1} k_{p2}}{s + k_m(k_{\theta 2} + k_{p2})} - \frac{k_m k_{p1} k_{\theta 2} + k_{p1} s}{s + k_m(k_{\theta 2} + k_{p2})}\left(\frac{k_o}{\tau_{ct}s + 1}\right)\right]\Delta\theta \Rightarrow \\ \Delta\dot{m}_{cyl} &= k_m k_{p2}\frac{(k_{\theta 1}\tau_{ct} - k_o\frac{k_{p1}}{k_m k_{p2}})s + (k_{\theta 1} - k_o k_{\theta 2}\frac{k_{p1}}{k_{p2}})}{(\tau_{ct}s + 1)[s + k_m(k_{\theta 2} + k_{p2})]}\Delta\theta. \end{aligned}$$

The block diagram of the linear IEGR system is shown in Figure 8. For simplicity we rewrite Eq. 4. in

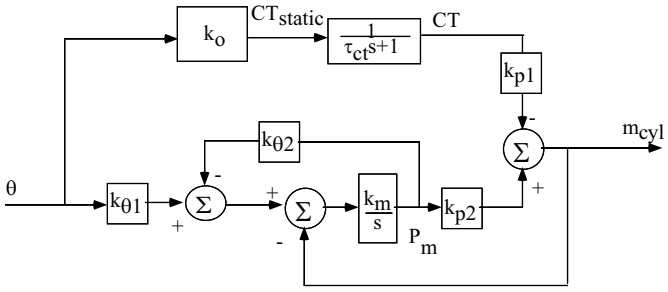

Figure 8: Block diagram of the linear IEGR system.

terms of its DC gain (k_{dc}), zero (z), and poles (p):

$$\Delta\dot{m}_{cyl} = k_{dc}\frac{\frac{s}{z}+1}{(\frac{s}{p_{ct}}+1)(\frac{s}{p_m}+1)}\Delta\theta \qquad (9)$$

where, $k_{dc} = \frac{k_{p2}k_{\theta 1}-k_{p1}k_{\theta 2}k_o}{k_{\theta 2}+k_{p2}}$, $z = \frac{k_{\theta 1}-k_o k_{\theta 2}\frac{k_{p1}}{k_{p2}}}{k_{\theta 1}\tau_{ct}-k_o\frac{k_{p1}}{k_m k_{p2}}}$, $p_{ct} = \frac{1}{\tau_{ct}}$, and $p_m = k_m(k_{\theta 2}+k_{p2})$. The poles $p_1 = -p_m$ and $p_2 = p_{ct}$ of this stable system are located at the right half plane (RHP). The zero $-z$ can be found to the left half as well as the open right half plane.

Proposition: The necessary and sufficient condition for the step response of (9) to be monotonic is

$$z \geq \min\{p_m, p_{ct}\}. \qquad (10)$$

This result follows from the general conditions for the monotonic step response, see [Jayasuriya et. al. 1996]. We use the notation $p_m(\theta, N)$, $z(\theta, N, \tau_{ct})$, $p_{ct}(\tau_{ct})$ to indicate the dependence of the poles and zeros of the IEGR engine transfer function on the operating point and the dynamic schedule. For small values of τ_{ct}, we have a non-minimum phase zero ($z < 0$) if $k_o > 0$. This follows because $1 - k_o\frac{k_{\theta 2}}{k_{\theta 1}}\frac{k_{p1}}{k_{p2}}$ is positive since $1 - k_o\frac{k_{\theta 2}}{k_{\theta 1}}\frac{k_{p1}}{k_{p2}} = \frac{k_{dc}}{k_{p2}k_{\theta 1}}$, and the static schedule ensures $k_{dc} > 0$ for all engine conditions. As τ_{ct} increases, the zero z converges to the origin at a rate equal to $1/(1 - k_o\frac{k_{\theta 2}}{k_{\theta 1}}\frac{k_{p1}}{k_{p2}}) < 1$. The pole p_{ct} converges to the origin slower, at a rate equal to 1. Hence, for large values of τ_{ct} the zero z is to the right of the pole p_{ct}, and torque exhibits an overshoot. Thus the admissible range for τ_{ct} that guarantees monotonic step responses is a bounded interval that can be computed from Eq. 9-10.

To summarize and relate the above analysis to the physical system consider the following scenarios. If an aggressive IEGR dynamic schedule has to be implemented to reduce feedgas emissions, the small time constant τ_{ct} might cause torque response to undershoot during step throttle changes (dot-dashed line in Fig. 9). If hardware limitations impose bandwidth constraints in the dynamic IEGR response, then the large time constant τ_{ct} might cause torque response to overshoot (zero to the right of the largest pole p_{ct}, solid line in Fig. 9), or to respond slowly to the torque demand due to the dominant slow pole p_{ct} (dashed line in Fig. 9). These conclusions hold in the region where the static schedule calls for cam phasing increase in response to throttle angle increase ($k_o > 0$).

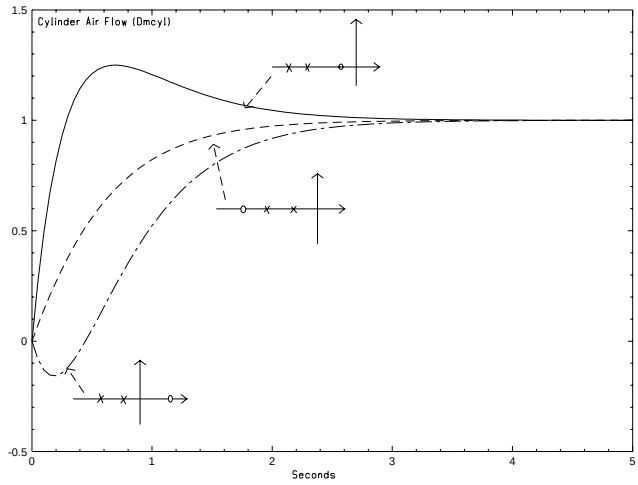

Figure 9: Qualitative cylinder air flow behavior of the IEGR system for different pole zero location.

In the region of high manifold pressure (normal flow, $k_{\theta 2} > 0$) the static schedule requires $k_o < 0$, i.e. we start decreasing the dilution to achieve the maximum engine torque (see Section 3.). In this case it can be verified that admissible values for τ_{ct} must be either sufficiently large or sufficiently small.

5. Target Transient Torque Response

Using appropriate values of the time constant of the first order lag (τ_{ct}) we seek to minimize the differences between the cylinder air flow transients of an IEGR engine and an engine with zero EGR. The target dynamic response is given by the transfer function from throttle angle to cylinder air flow for an engine with zero EGR. This transfer function can be found by linearization of Eq. 4 after setting IEGR and consequently camshaft timing equal to zero ($CT = 0$):

$$\Delta\dot{m}_{cyl} = \frac{k_m k_{\theta 1}k_{p2}}{s + k_m(k_{\theta 2}+k_{p2})}\Delta\theta\ . \qquad (11)$$

Note here that Eq. 11 can be derived also from Eq. 4. by assigning k_{p1} equal to zero. We can compare the two dynamical systems after we rewrite the above transfer function with respect to its DC gain and pole location:

$$\Delta\dot{m}_{cyl} = \tilde{k}_{dc}\frac{1}{\frac{s}{p_m}+1}\Delta\theta \qquad (12)$$

where, $\tilde{k}_{dc} = \frac{k_{p2}k_{\theta 1}}{k_{\theta 2}+k_{p2}}$, and p_m as given in Eq. 9.

The following table summarize the differences between the closed loop transfer functions from throttle to cylinder air flow for the IEGR system and the zero EGR (ZEGR) system:

	ZEGR Engine	IEGR Engine
DC Gain	$\tilde{k}_{dc}=\frac{k_{\theta 1}k_{p2}}{k_{\theta 2}+k_{p2}}$	$k_{dc}=\frac{k_{\theta 1}k_{p2}-k_o k_{p1}k_{\theta 2}}{k_{\theta 2}+k_{p2}}$
Transfer Function	$\frac{\Delta \dot{m}_{cyl}(s)}{\Delta\theta(s)}=\tilde{k}_{dc}\frac{1}{\frac{s}{p_m}+1}$	$\frac{\Delta \dot{m}_{cyl}(s)}{\Delta\theta(s)}=k_{dc}\frac{\frac{s}{z}+1}{(\frac{s}{p_m}+1)(\frac{s}{p_{ct}}+1)}$

where $p_m = k_m(k_{\theta 2}+k_{p2})$, $p_{ct}=\frac{1}{\tau_{ct}}$, and $z=\frac{k_{\theta 1}-k_o k_{\theta 2}\frac{k_{p1}}{k_{p2}}}{k_{\theta 1}\tau_{vct}-k_o\frac{k_{p1}}{k_m k_{p2}}}$.

As expected, the IEGR engine has considerably smaller DC gain than the ZEGR engine. Its DC gain depends on the static camshaft timing schedule ($k_o > 0$) during subsonic flow ($k_{\theta 2} \neq 0$). Although the target response is the ZEGR engine, we cannot match the DC gain of the ZEGR engine and there is no need to do so. The IEGR engine can meet the torque demand at higher throttle angle. Doing so will be beneficial to fuel economy due to reduction in pumping losses [Stein et. al. 1995].

The differences in the dynamic characteristics of the two systems are due to the zero z and the additional pole p_{ct}. The zero is the result of the interaction of the IEGR dynamics with the manifold filling dynamics. The pole is due to the the first order lag of the dynamic schedule. We seek to eliminate the combined effects of the zero z and the additional pole p_{tc} in the IEGR torque response so that the IEGR transient behavior is similar to the ZEGR engine.

6. Optimization

To obtain acceptable torque responses for the IEGR engine, τ_{ct} needs to be adjusted as engine operating conditions change. To achieve this we use a nonlinear static map of the form:

$$\tau_{ct}(t) = \mathcal{T}(\theta(t), N(t)). \tag{13}$$

This map has been generated to achieve the monotonicity (10), and, whenever possible, the complete matching between the IEGR and the ZEGR step response (modulo dc values) at particular operating points of throttle angle and engine speed. The time constant τ_{ct} is expressed as a function of engine cycles to facilitate event-based real-time controller implementation. The resulting nonlinear static map is shown in Figure 10. Note that the specific procedure for generating $\mathcal{T}$ is fairly involved computationally. However, these computations are off-line and the on-line implementation of (13) is straightforward. A lookup table and linear interpolation are used to interpolate between the discrete values of $\mathcal{T}$ as computed for the discrete set of pairs (θ, N).

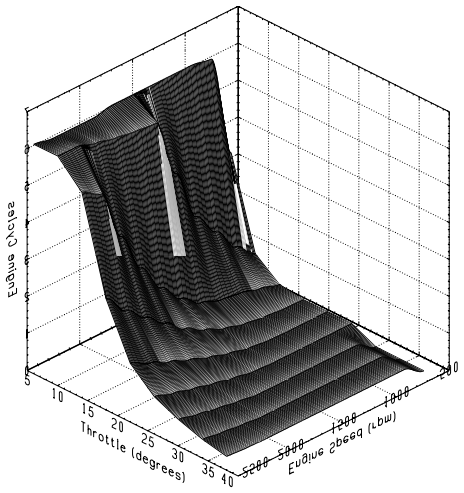

Figure 10: The selected time constant τ_{ct} for different throttle angles and engine speeds.

7. Results

In this section we test the nonlinear map $\mathcal{T}$ using a nonlinear simulation engine model equipped with variable camshaft timing and coupled with vehicle dynamics. Throughout the simulation we use stoichiometric air-to-fuel ratio (A/F=14.64), minimum spark advance for best torque ($\sigma = \sigma_{MBT}$), and fourth gear at the modeled automatic transmission. The throttle steps used represent a series of challenging torque demands and test the engine behavior over a wide operating range. The ZEGR engine ($ZEGR$, solid line in Fig 11) provides the benchmark torque response for evaluating the dynamically schedulled IEGR engine. Figure 11 also shows the simulation of the IEGR engine using the developed static camshaft schedule (CT_{static}) and three different transient characteristics: (i) time constant τ_{ct} determined by the nonlinear map $\mathcal{T}$ ($IEGR(opt)$, dashed line), (ii) time constant τ_{ct} was chosen to be equal to one engine cycle for all operating condition ($IEGR(1cycle)$, dotted-dashed line); and (iii) time constant τ_{ct} was chosen to be equal to six engine cycles for all operating condition ($IEGR(6cycles)$, dotted-dotted-dashed line). Testing the three different IEGR schemes will provide a measure of performance degradation when memory or computing power constraints impose limitations in implementing the fully nonlinear map $\mathcal{T}$.

The differences between the cylinder air flow of ZEGR engine and the IEGR engines are shown in the fifth row of Fig. 11. The subtle differences between the different IEGR dynamic scheduling schemes can be evaluated if we look closer in the A, B, and C areas of the nonlinear simulation.

Figure 12 magnifies the A, B and C areas of the nonlinear simulation shown in Fig 11. At $t = 2$ sec. (plot A) a small increase in throttle causes the slow IEGR system to exhibit overshoot and the fast IEGR system to

exhibit undershoot in the cylinder air flow response. The IEGR engine that uses the time constant as defined by the nonlinear map $\mathcal{T}$ has a smooth response.

At $t = 8$ sec. (plot B) a large throttle increase causes camshaft timing to return to base camshaft timing (0 degrees). The IEGR engines that manage to do so at a fast rate (both $IEGR(opt)$ and $IEGR(6cycles)$) have similar response to the ZEGR engine, whereas the slow IEGR system varies significantly from the target response.

At $t = 10$ sec. (plot C) a decrease in throttle angle requires camshaft timing to attain its maximum value (see fourth row of Fig. 11). During this step change, the fast IEGR system and the slow IEGR system ($IEGR(1cycle)$ and $IEGR(6cycles)$ respectively) overshoot or respond slowly to the change in torque demand. The response achieved by the IEGR engine that uses the nonlinear static map $\mathcal{T}$ matches the ZEGR dynamic response.

Figure 13 shows the brake torque (second row) and the vehicle velocity (third row) of the ZEGR and the three IEGR engines for the same throttle steps as in Fig. 11. As expected, the simulated brake torque resembles the cylinder air flow response justifying the assumptions made in Section 4..

8. Conclusions

Extensive simulations of the developed IEGR dynamic scheduling scheme demonstrate its ability to match the dynamic response of a ZEGR engine. The scheme comprises of a steady-state map used as set points of a tracking problem and a first order lag that defines the transition between the optimal steady-state points. Both the steady-state set point and the time constant of the first order lag depend on nonlinear static maps of throttle angle and engine speed, CT_{static} and $\mathcal{T}$ respectively. We investigated two other suboptimal dynamic schedules for the IEGR engine with the goal to demonstrate the subtle but potentially important deterioration of the engine's torque response if $\mathcal{T}$ is not used.

9. Acknowledgment

The authors wish to acknowledge Professor James Freudenberg for the helpful discussions and Kenneth Butts for the vehicle simulation model; Tom Leone and Mark Seaman for the impeccable experimental data; and Ed Badillo for the invaluable comments on drivability and engine performance.

References

[Jayasuriya et. al. 1996] Jayasuriya, S., and Song, J.-W., 1996, "On the Synthesis of Compensators for Nonovershooting Step Response," *ASME Journal of Dynamic Systems, Measurement, and Control*, vol. 118, pp. 757-763.

[Stefanopoulou et. al. 1995] Stefanopoulou, A.G., Cook, J.A., Freudenberg, J.S., Grizzle, J.W., Haghgooie, M., and Szpak, P.S., 1995, "Modeling and Control of a Spark Ignition Engine with Variable Cam Timing," *1995 American Control Conference*, Seattle.

[Stein et. al. 1995] Stein, R.A., Galietti, K.M., and Leone, T.G., 1995, "Dual Equal VCT- A Variable Camshaft Timing Strategy for Improved Fuel Economy and Emissions," SAE Paper No. 950975.

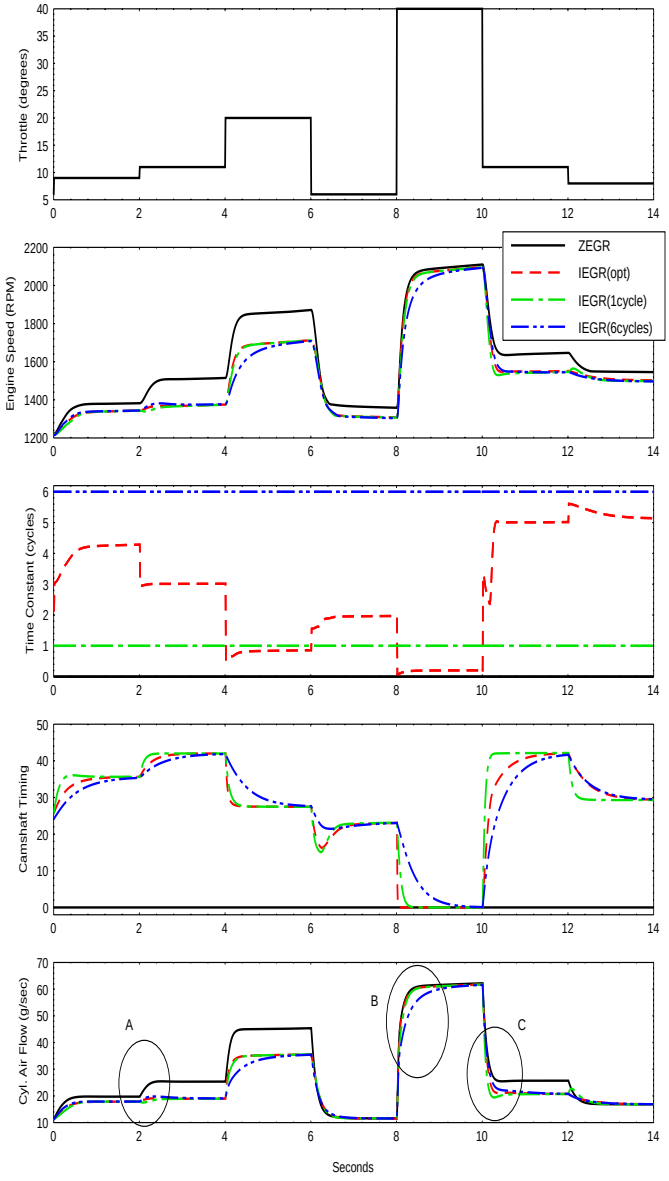

Figure 11: Nonlinear simulation of (i) the zero EGR system (ZEGR), (ii) the IEGR system with the optimized time constant (τ_{ct}), (iii) the IEGR system for a small time constant ($IEGR(1cycle)$), and (iv) the IEGR system for a large time constant ($IEGR(6cycles)$).

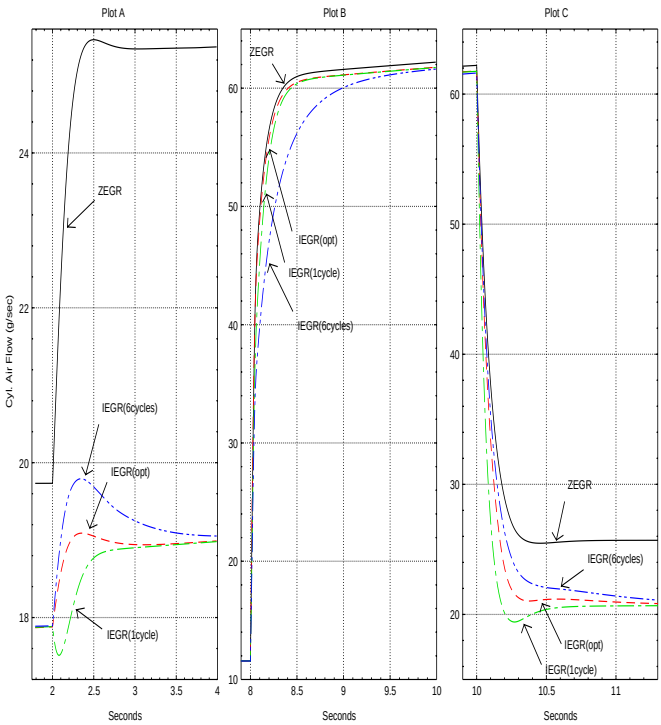

Figure 12: Dynamic behavior of mass air flow of the four different systems ($ZEGR$, $IEGR(opt)$, $IEGR(1cycle)$, and $IEGR(6cycles)$) during throttle steps .

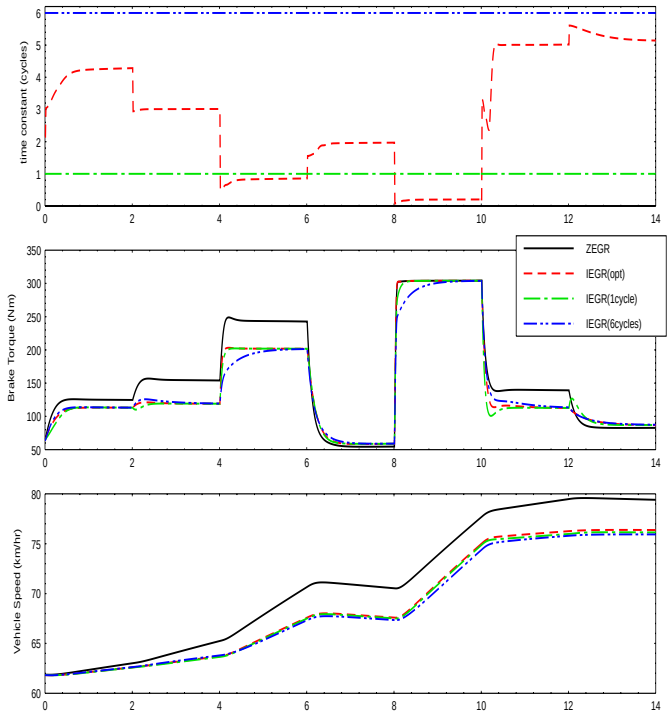

Figure 13: Nonlinear simulation of the four different systems ($ZEGR$, $IEGR(opt)$, $IEGR(1cycle)$, and $IEGR(6cycles)$) during throttle steps after introducing vehicle dynamics.